

# Radiographic Determinants of the Elbow Rotation Axis: Experimental Identification and Quantitative Validation

\*M. Bottlang, †M. R. O'Rourke, §S. M. Madey,  
†C. M. Steyers, †J. L. Marsh, and †‡T. D. Brown

\*Biomechanics Laboratory, Legacy Clinical Research and Technology Center, Portland; Departments of  
†Orthopaedic Surgery and ‡Biomedical Engineering, University of Iowa, Iowa City, Iowa; and  
§Department of Trauma Surgery, Legacy Emanuel Hospital, Portland, Oregon, U.S.A.

**Summary:** This study identifies new radiographic indices to approximate the location of the elbow rotational axis. With use of electromagnetic motion tracking source data, the average rotational axis of the ulnohumeral articulation was calculated in seven cadaveric specimens. Quasi-lateral radiographs of the elbow specimens were then analyzed to identify radiographic landmarks of the elbow axis in the lateral view. The spatial relationships of these landmarks with the elbow aligned on-axis were contrasted with their relationships in eight distinct off-axis alignments. Elbow axis orientation in the transverse plane (internal/external rotation) was identified by the location of a dense intramedullary cortical line, appearing in the projection of the distal humerus in relation to the periosteal surface of the posterior cortex of the humerus. This intramedullary line corresponds to the posteromedial cortex of the distal humerus. Correct alignment occurred when this line laid  $27.1 \pm 3.7\%$  of the anteroposterior humeral diameter anterior from the periosteal surface of the posterior cortex. Axis orientation in the coronal plane (abduction/adduction) was identified by the concentric appearance of radiographic arcs formed by the capitellum, trochlear sulcus, and medial trochlear flange. Using these radiographic indices, three orthopaedic surgeons were able to fluoroscopically align the elbow along the axis of rotation with an accuracy of  $3.7 \pm 1.8^\circ$ . These results are immediately applicable to fluoroscopic identification of the elbow axis. This technique can be used to increase the accuracy of hinge placement during application of hinged external fixation or distraction arthroplasty.

The elbow functions essentially as a hinge (2,4,6,7,12,14,15,20-23) and therefore lends itself well to the use of articulated external fixation. In a number of clinical circumstances, application of such a fixator would seemingly improve stability, allow for early motion, prevent soft-tissue contracture, and improve range of motion (8-11,13,18). Indications include complex fractures around the elbow and the surgical management of joint stiffness or ankylosis.

Several articulated fixators have been described (6,10,16,17,19,22). Clinical results have been encouraging, but the complication rates have been as high as 40-50% (13,24). Specific problems include pin loosening and breakage, infection, recurrent instability, and nerve injury. Off-axis alignment of the external fixator may be responsible, at least in part, for the high complication rate (4). Previous work in our laboratory has shown that the fixator hinge must be accurately aligned with the elbow axis to minimize extra

resistance to joint motion caused by the fixator application. Off-axis alignment between the fixator hinge and the elbow axis in the transverse and coronal planes led on average to a 3.7 and 7.1-fold increase in motion resistance for 5 and 10° mal-orientation, respectively (4). This large increase in motion resistance when the fixator is misaligned may elevate stress at the bone-pin interface and lead to abnormal forces and bending moments at the elbow joint.

Application of the fixator itself is technically demanding (13,24). Most articulated elbow fixators have medial and lateral hinges or require placement of an axis pin through the distal humerus, or both. The criteria conventionally used to identify the elbow axis (lateral epicondyle and the anteroinferior aspect of the medial epicondyle) are relatively nonspecific. Furthermore, given the narrow margin of error apparently allowable for fixator alignment along the physiological axis, the potential for error in the placement of the axis pin is sizable. The axis pin is usually drilled from the medial anteroinferior aspect of the medial epicondyle to the tubercle of the lateral epicondyle (6,10,17). The entry site at the medial epicondyle is not perpendicular to the elbow axis, which

Received June 7, 1999; accepted January 10, 2000.

Address correspondence and reprint requests to M. Bottlang at Biomechanics Laboratory, Legacy Clinical Research and Technology Center, 1225 NE 2nd Avenue, Portland, OR 97232, U.S.A. E-mail: mbottlan@lhs.org

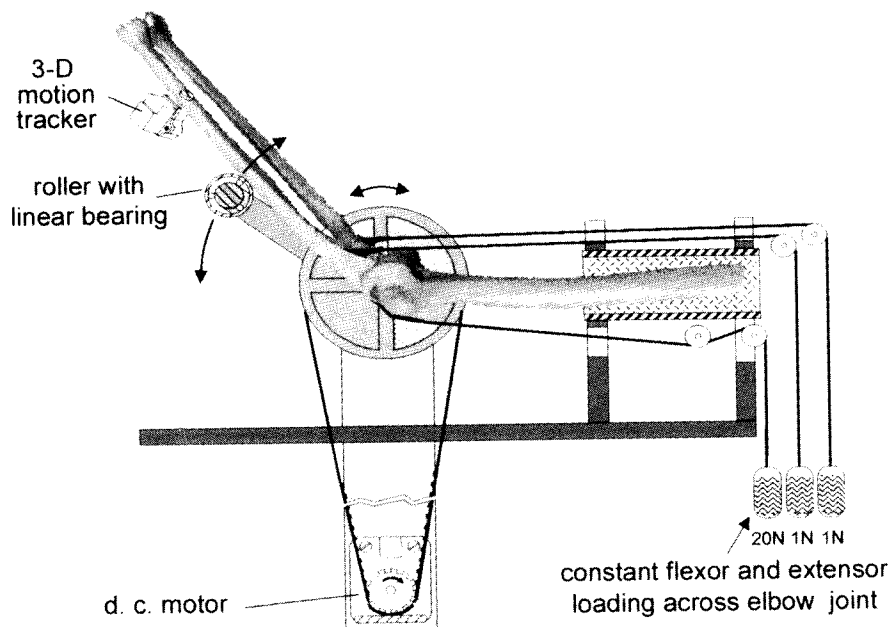


FIG. 1. Test setup (drawing not to scale) for the application and acquisition of minimally constrained passive elbow motion.

may cause skewing and resultant misplacement of the entry point. Once the axis pin tract is initiated, errors in orientation are difficult to correct and are likely to be exacerbated by pin migration.

Many of these problems might be avoided by the use of radiographic landmarks to orient an articulated fixator along the elbow axis without the necessity for placement of an axis pin. Prior to a thorough investigation of elbow kinematics (3,5), we attempted to de-

termine novel and improved radiographic indices that can be used to identify the elbow axis accurately. Following identification and quantification of reliable indices, we tested our ability to identify the elbow axis on the basis of these indices using fluoroscopy in a simulated clinical setting.

## MATERIALS AND METHODS

Seven fresh-frozen cadaveric upper extremities with no radio-

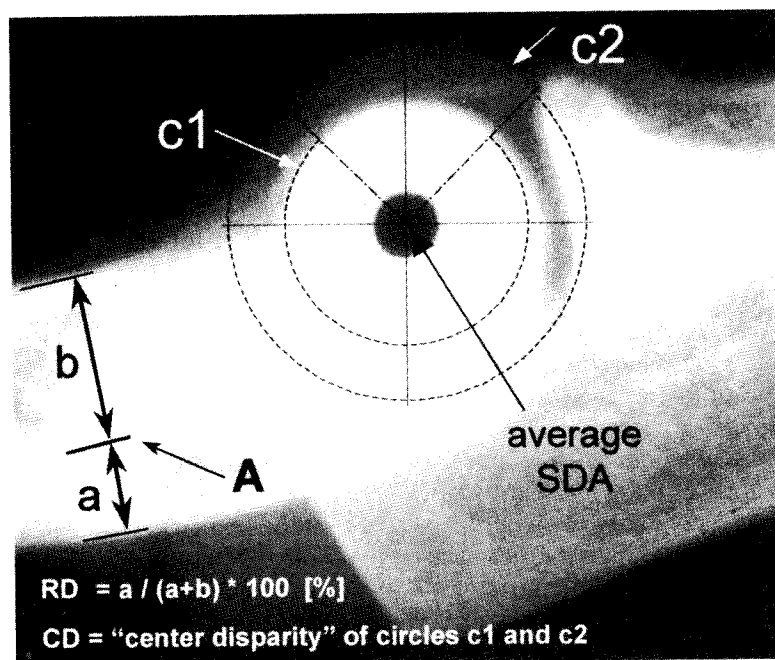
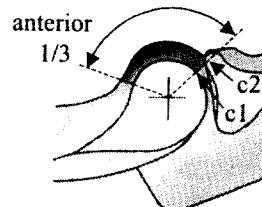
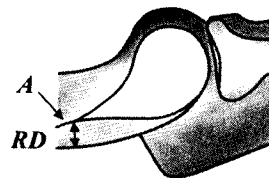
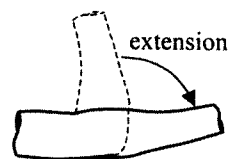


FIG. 2. Radiographic appearance of the elbow, with an x-ray beam sitting precisely along the average screw displacement axis (SDA). This on-axis view is characterized by (a) the location of a dense cortical line (A) with respect to the posterior border of the humerus, quantified as relative distance (RD), and (b) the concentric appearance of two circular shadows, formed by the superimposed capitellum and trochlear sulcus (c1) and the medial flange of the trochlea (c2), quantified as center disparity (CD).

## Sequential Elbow Alignment Protocol

- 1 Quasi-lateral fluoroscopic visualization of
  - elbow in full extension
- 2 Adjustment of  $RD \approx 27\%$  by
  - internal or external humeral rotation
  - utilizing criterion *A*
- 3 Adjustment of  $CD \approx 0$  mm by
  - humeral ab- or adduction
  - utilizing anterior 1/3 of *c1*, *c2*
  - decreasing x-ray exposure (if necessary)



**FIG. 3.** Sequential elbow alignment protocol used to quantitatively evaluate the accuracy of the index-based elbow axis detection procedure.  $RD$  = relative distance and  $CD$  = center disparity.

graphic or visual evidence of pathologic conditions were prepared for testing in a custom-designed motion applicator. Skin, subcutaneous tissues, and muscles were excised, while the joint capsule, ligaments, and musculotendinous insertions were retained. The test fixture induced minimally constraining passive motion to the elbow joint without manual interference at a constant angular velocity of  $32^\circ/\text{sec}$  (Fig. 1). The kinematics of rotation around the elbow joint were recorded with an electromagnetic tracking system (Flock of Birds, model 6DFOB; Ascension Technology, Burlington, VT, U.S.A.). The motion tracking data, expressed in terms of the screw displacement axis calculated by Beggs' (1) algorithm in combination with a customized source data smoothing procedure (2), were used to completely describe the three-dimensional

kinematics of the ulna with respect to the humerus. For each specimen, an average screw displacement axis was calculated by averaging all screw displacement axes obtained over a range of motion of  $10$ - $130^\circ$ . This average screw displacement axis was physically marked in each specimen by drilling a corresponding  $4$ -mm hole into the distal humerus (6). We then visualized the location of the average screw displacement axis with respect to the longitudinal axis of the humerus and ulna in an anteroposterior fluoroscopic view. To establish criteria on the lateral radiograph, the distal humerus was viewed with the x-ray beam oriented precisely along a  $150$ -mm-long metal tube with a  $1.5$ -mm inner diameter that was inserted into each specimen along the calculated average screw displacement axis. With this technique, the calculated average

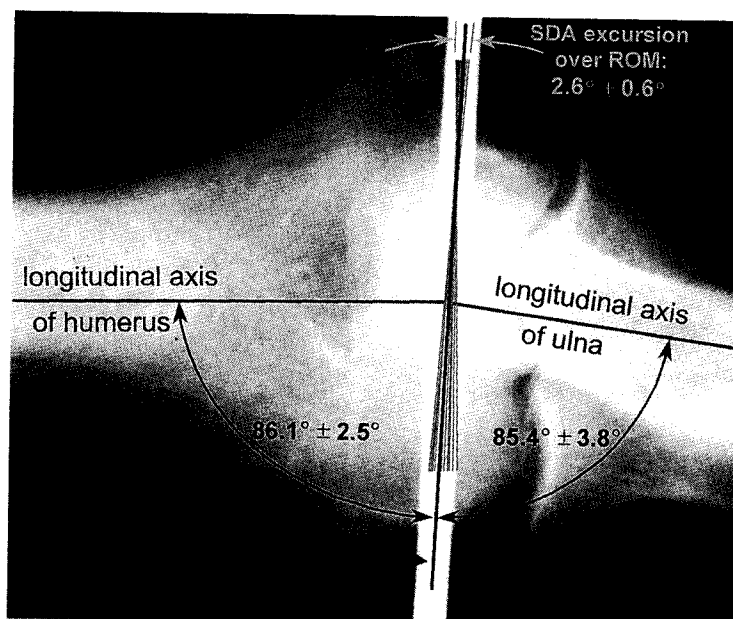


**FIG. 4.** Excursion of the instantaneous screw displacement axis (SDA) (range of motion [ROM] from  $10$  to  $130^\circ$ ) and location of the calculated average screw displacement axis, shown in the coronal plane. The average screw displacement axis penetrates the anteroinferior aspect of the medial epicondyle, the center of the trochlea, and the center of the projection of the capitellum onto a parasagittal plane.

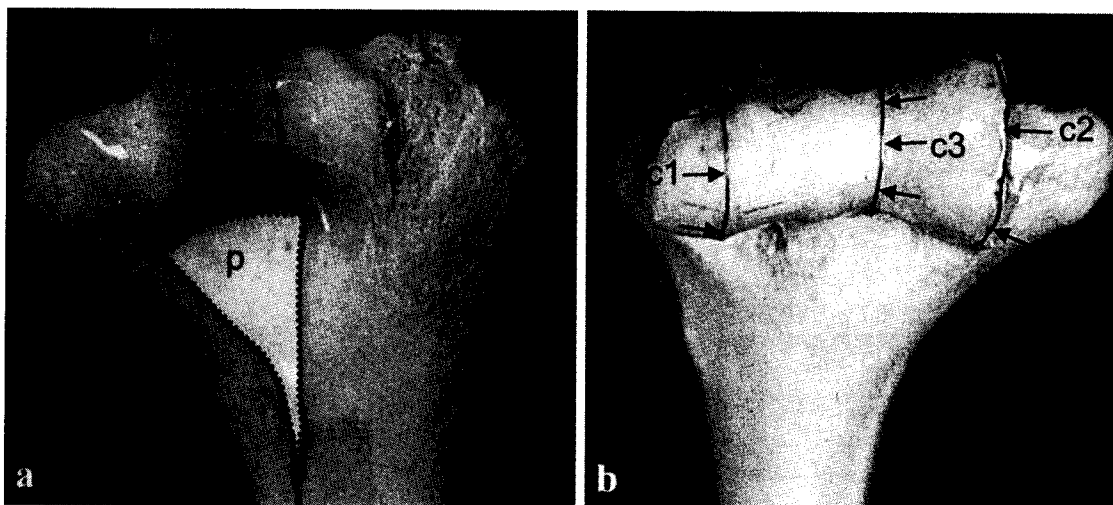


**FIG. 5.** Lead marker study, relating anatomical landmarks to the radiographic indices RD (relative distance) and CD (center disparity). **a:** Relative distance is based on the projections of a flat cortical plate (p) of the posteromedial aspect of the distal humerus onto the radiodense line A. **b:** Center disparity is based on two apparently concentric circular radiographic shadows formed by the superimposed capitellum (c1) and trochlear sulcus (c3) and the medial flange of the trochlea (c2).

screw displacement axis was radiographically identified with an accuracy of greater than  $0.6^\circ$  on the basis of the geometry of the tube lumen.

Quasi-lateral radiographs were obtained with the humerus in on-axis orientation as well as in eight distinct off-axis orientations with respect to the x-ray beam (humerus angulated  $5^\circ$  and  $10^\circ$  toward abduction/adduction and external/internal rotation). These radiographs were systematically analyzed to identify two prominent landmark-based criteria that were most sensitive to the two independent components of elbow off-axis alignment. The radiographic criteria identified were (a) the position of a dense cortical line apparent in the distal humerus and (b) the concentricity of circular shadows apparent at the humeral articular surface. These circular shadows were consistently visible over an arc of  $90\text{--}130^\circ$  at the anterior articular surface. The osseous structures correlating to these radiographic criteria were determined by sequentially

marking areas on the distal humerus with fine lead wire and obtaining radiographs in on-axis and off-axis orientations.

To enable quantification of the sensitivity of the radiographic criteria to known amounts of elbow off-axis alignment, we established two radiographic indices: RD (relative distance) and CD (center disparity). The location of the radiodense line (A) with respect to the posterior border of the humerus was quantified as relative distance (RD, Fig. 2). The relative distance was measured along a line perpendicular to the longitudinal axis of the humerus at the junction of the proximal aspect of the olecranon fossa and the projection of the posteromedial cortical plate (Fig. 6). The concentric appearance of the circular shadows (c1 and c2, Fig. 2) was quantified by means of the center disparity. Two circles were fit to the circular shadows by digitizing points on the anterior portion of each shadow. The concentricity was then quantified by the center disparity between the centers of the two fitted circles.

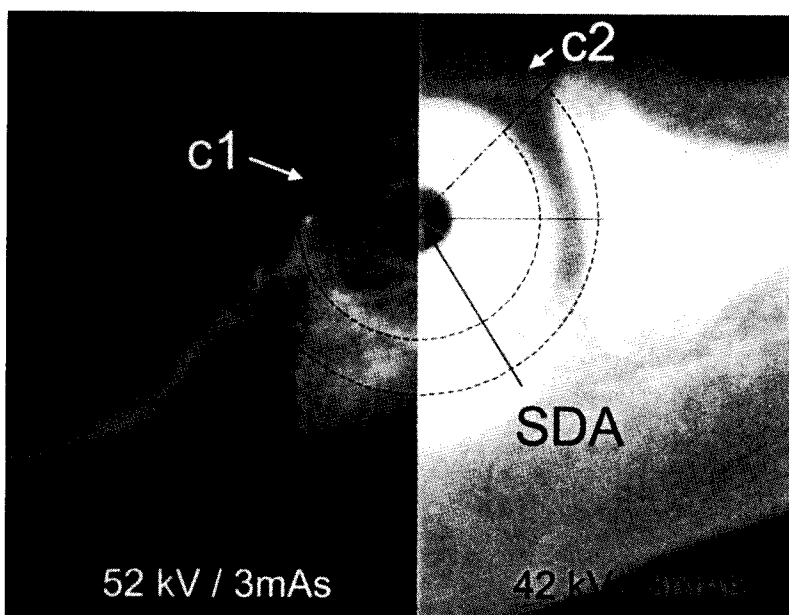


**FIG. 6.** The medial trochlear facet (c2) was not pronounced on x-rays obtained at high exposure intensity (52 kV/3 mA). Decreasing the x-ray exposure intensity to 42 kV/3 mA drastically improved the visibility of the medial trochlear facet (c2) without having a reverse negative effect on the pronounced appearance of the periphery of the capitellum (c1).

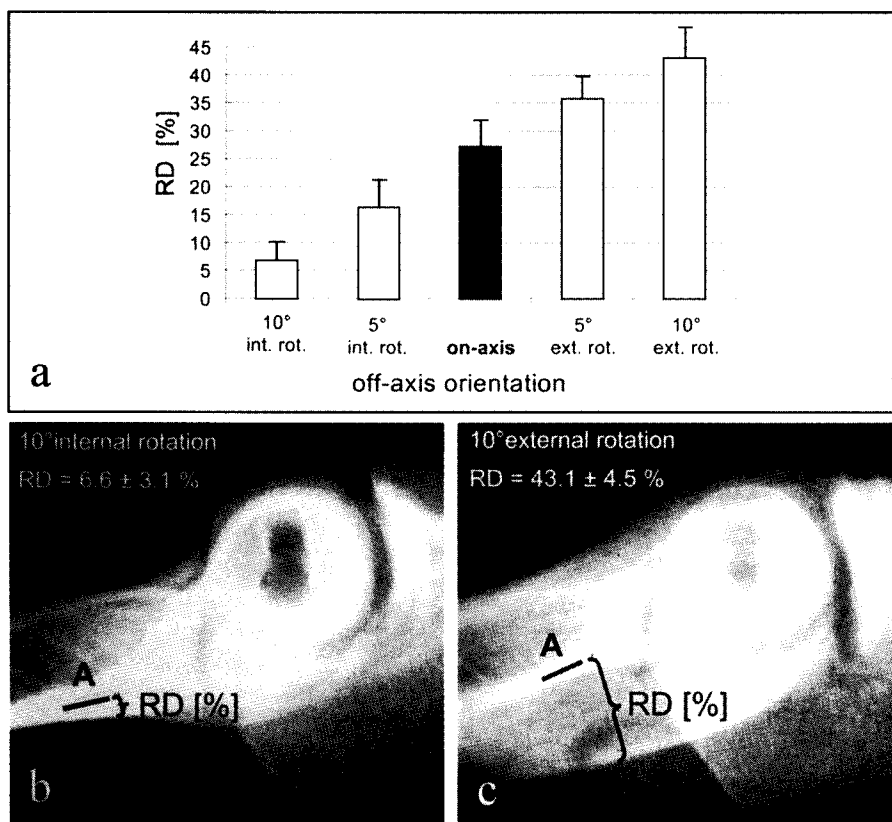


**FIG. 7. a:** Sensitivity of the radiographic landmark A, quantified by the relative distance (RD), toward elbow off-axis orientation due to internal or external rotation of the humerus. **b:** Ten degrees of internal humeral rotation projects landmark A to be quasi-coincident with the posterior humeral cortex (RD = 6.6 ± 3.1%). **c:** 10° of external rotation shifted landmark A toward the center of the intramedullary channel (RD = 43.1 ± 4.5%).

where center disparity = 0 mm depicts perfectly concentric circles.

We then tested our ability to use these radiographic indices to detect the elbow axis under fluoroscopic visualization in a simulated clinical setting. The seven cadaveric specimens were mounted in a positioning device made of Plexiglas. This positioning device allowed gradual and controlled changes of orientation in a single plane (abduction/adduction and internal/external rotation). To prevent the introduction of bias, barium paste was utilized to completely obscure the physically inserted axis without impairing the visibility of the radiographic landmarks (*A*, *c1*, and *c2*). Three orthopaedists, a trauma surgeon (J.L.M.), a hand surgeon (C.M.S.), and an orthopaedic surgery resident (M.R.O.), individually attempted to identify the axis under fluoroscopic visualization using the indices relative distance and center disparity according to a sequential elbow alignment protocol (Fig. 3). Each observer aligned the seven elbow specimens first by obtaining alignment in the transverse plane (i.e., internal/external rotation) by positioning the radiodense line (*A*) according to relative distance values of 25-30%. Alignment in the coronal plane (i.e., abduction/adduction) was then approached by maximizing the concentricity of the radiographic circles (*c1* and *c2*) (thus minimizing the center disparity). After the axis of each specimen was identified, the orthopaedists left the suite and the deviation from the previously calculated axis was accessed from the scales of the positioning device. The orthopaedists were not informed of the results until all the specimens were evaluated.

## RESULTS

The instantaneous screw displacement axes corresponding to a range of motion from 10 to 130° nearly

intersected at the medial flange of the trochlea (Fig. 4). The calculated average screw displacement axis penetrated the anteroinferior aspect of the medial epicondyle, the center of the trochlea, and the center of the projection of the capitellum onto a parasagittal plane. For a fully extended elbow viewed in the coronal plane, the average screw displacement axis formed angles of  $86.1 \pm 2.5$  and  $85.4 \pm 3.8^\circ$  (mean  $\pm$  SD) with the longitudinal axes of the humerus and ulna, respectively.

The lead-marker study revealed that the radiodense line (*A*) corresponds anatomically to a flat cortical plate (*p*) on the posterolateral aspect of the distal humerus, lateral to the olecranon fossa and extending proximally to include the lateral supracondylar ridge (Fig. 5a). The two circular shadows (*c1* and *c2*), apparent in the on-axis projection, are formed by the superimposed capitellum and trochlear sulcus (*c1* and *c3*) and the medial flange of the trochlea (*c2*) (Fig. 5b).

The lateral radiographic view along the average screw displacement axis was characterized by means of two radiographic indices: RD (relative distance) and CD (center disparity). The on-axis radiograph projects the radiodense line (*A*) anterior to the posterior border of the humerus by  $27.1 \pm 3.7\%$  (relative

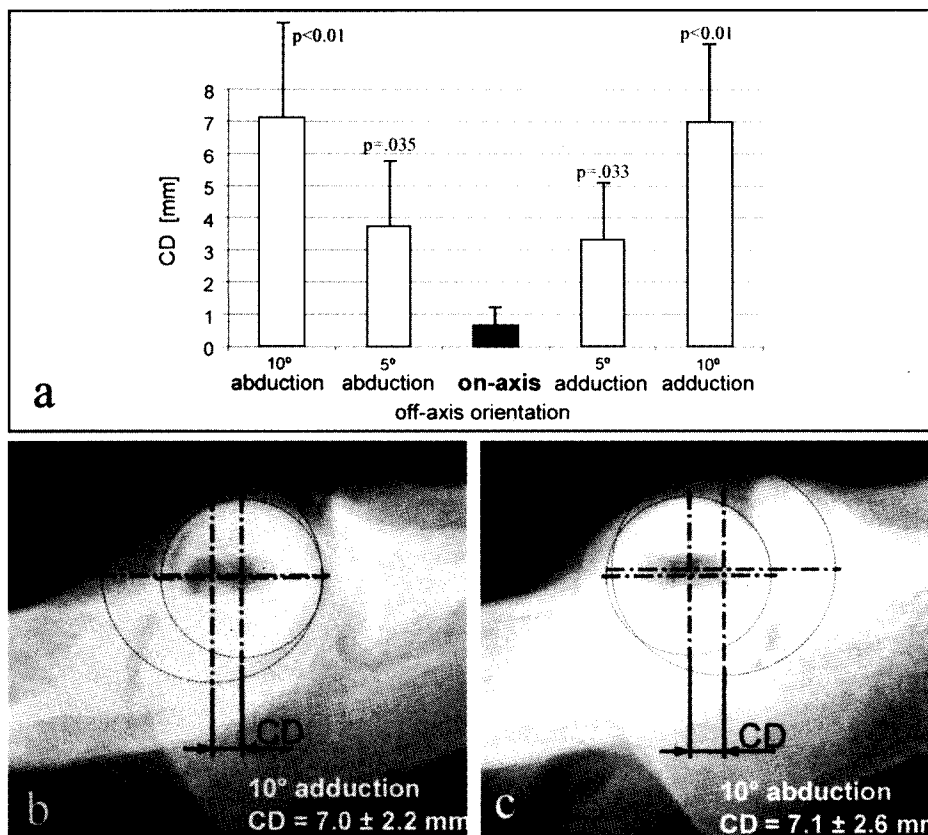


**FIG. 8.** Sensitivity of the concentric appearance of the periphery of the capitellum and the medial trochlear facet, quantified by the center disparity (CD), toward elbow off-axis orientation due to adduction/abduction of the humerus. **a:** The on-axis aligned elbow yielded in concentric circles with CD values of  $0.5 \pm 0.6$  mm. **b** and **c:** The center disparity is highly sensitive toward humeral off-axis abduction and adduction. Ten degrees of adduction or abduction corresponds to CD values of  $7.0 \pm 2.2$  and  $7.1 \pm 2.6$  mm, respectively.

distance) of the anteroposterior diameter of the humerus. Furthermore, on-axis radiographs were characterized by apparently concentric circular shadows formed by the medial trochlear flange and the superimposed trochlear sulcus and capitellum, corresponding to center disparity values of  $0.5 \pm 0.6$  mm. In two of seven elbow specimens, the medial trochlear flange was difficult to see under standard exposure (52 kV/3 mA). Visualization was improved by decreasing the exposure (42 kV/3 mA) without compromising the clarity of the capitellum (Fig. 6).

The sensitivity analysis revealed a nearly linear relationship between relative distance and the amount of off-axis orientation due to internal or external rotation of the humerus (Fig. 7a). Ten degrees of internal rotation projected line A to a position quasi-coincident with the posterior humeral cortex (relative distance =  $6.6 \pm 3.1\%$ ) (Fig. 7b). Ten degrees of external rotation shifted line A toward the center of the intramedullary channel (relative distance =  $43.1 \pm 4.5\%$ ) (Fig. 7c). Therefore, relative distance quantifies an index sensitive to axial alignment in the transverse plane (i.e., internal/external rotation). The center disparity was significantly increased ( $p < 0.035$ , two-tailed heteroscedastic two-sample *t* test) for humeral

off-axis adduction and abduction as small as  $5^\circ$  (Fig. 8a). Ten degrees of adduction or abduction corresponded to center disparity values of  $7.0 \pm 2.2$  and  $7.1 \pm 2.6$  mm, respectively (Fig. 8b and c). Therefore, the center disparity index proved extremely efficient in determining the correct axial alignment in the coronal plane (i.e., adduction/abduction).

Using both the relative distance and center disparity indices under lateral fluoroscopic visualization, a trauma surgeon, a hand surgeon, and a junior orthopaedic resident were able to achieve alignment of the elbow joint along its rotation axis with an accuracy of  $3.7$ ,  $3.4$ , and  $4.1^\circ$ , respectively. On average, they achieved an accuracy of  $3.7 \pm 1.8^\circ$ . Their average off-axis alignments toward internal/external rotation and toward adduction/abduction were  $2.3 \pm 1.6$  and  $3.0 \pm 1.8^\circ$ , respectively. Repetitive alignment of the same specimen by each of the three observers yielded average errors ranging from  $1.8^\circ$  (specimen no. 2) to  $5.5^\circ$  (specimen no. 3).

## DISCUSSION

We identified novel landmarks of the elbow axis that are apparent on a single lateral radiograph. Landmark-derived criteria can be used to accurately detect

the elbow axis and thus can enable the surgeon to align an external hinge to the elbow rotation axis for optimum results. Using the two novel indices relative distance and center disparity, the two experienced orthopaedic surgeons, as well as the junior orthopaedic resident, achieved alignment of elbow specimens along their true axis with a relatively high degree of accuracy ( $3.7 \pm 1.8^\circ$ ).

Index relative distance reflects geometric relations measured in a sagittal plane projection. Therefore, relative distance is distinctively sensitive to internal/external elbow rotation but presumably is not affected by elbow abduction/adduction. Adjustment of relative distance prior to center disparity was necessary to ensure consistent visibility of radiographic landmarks for detection of center disparity.

Index center disparity is sensitive to internal/external rotation as well as to abduction/adduction. The reported sensitivity of center disparity to elbow abduction/adduction was obtained after adjustment of relative distance had been completed. The concentric shadows of the trochlea and capitellum used for assessment of center disparity demonstrate prominent visibility over arcs of approximately  $120^\circ$  at the anterior aspect of the joint, with the elbow in full extension. These arcs correspond to bone structures of the medial and lateral margins of the joint. The relatively large spatial separation of these joint margins qualifies the configuration of these arcs as a sensitive indicator of off-axis alignment in the coronal plane (i.e., abduction/adduction). Lowering the fluoroscopic exposure enhanced the visibility of the medial flange of the trochlea. There is appreciable variability in the appearance of the medial trochlear flange at the superior edge of the articular surface as it approaches the coronoid fossa; therefore, use of this transition region should be avoided when evaluating concentricity.

Our average screw displacement axis was calculated from  $10$  to  $130^\circ$  of elbow range of motion. The screw displacement axis at  $10^\circ$  actually utilizes data from  $7.5$  to  $12.5^\circ$ . Many of the specimens had variable amounts of slight flexion contractures, and therefore a complete data set was not available for the terminal  $10^\circ$  of extension. London (12) found sliding motion, as opposed to rotation, at the terminal  $10^\circ$  of flexion and extension. Von Meyer noted that the terminal flexion and extension were accompanied by external and internal axial rotation, respectively (23). Morrey and Chao (14) also found  $5^\circ$  of external and internal rotation with terminal flexion and extension, respectively. The consequences of deviation from hinge motion at terminal flexion and extension are not known. However, the range of motion for which hinge-type motion occurs is well within the functional range of motion for activities of daily living (15). The clinician

must use judgment when determining the range of motion tolerated with application of an external fixator.

The accuracy of our axis-detection procedure was established in an operating room setting, where the manual elbow alignment was compared with the average elbow axis, determined by the well established technique of screw displacement axis computation from data for three-dimensional joint kinematics (2). In addition, correlating the experimentally determined accuracy of this axis-detection procedure with the precision of those currently utilized is of great interest. We are not aware of other studies that have confirmed the accuracy of alternative axis-detection procedures or clinicians' interpretations of the elbow axis relative to a known axis derived from kinematic analysis. If the reported accuracy of axis detection is sufficient, clinical requirements will largely depend on the applied treatment.

London used a two-dimensional radiographic study (using a modification of Reuleaux's technique) to confirm that the plane of elbow flexion is defined by the plane of the trochlear sulcus and that the axis of elbow rotation passes through the center of the trochlea and the center of the capitellum (12). He oriented the x-ray beam along the axis of elbow rotation to obtain true lateral radiographs of the elbow, which showed three concentric arcs formed by the medial flange of the trochlea, the trochlear sulcus, and the capitellum. We found that only two such arcs are clearly visible when a lateral radiograph is aligned along the axis of rotation. When the lateral image was slightly off-axis, the trochlear sulcus and the capitellum could be seen variably as two distinct arcs. Morrey (17) described the insertion of an axis pin through the elbow to guide hinge alignment of a hinged elbow distractor. This widely adopted technique utilizes anatomical landmarks on the lateral and medial elbow aspect to direct pin insertion. Compared with the axis pin technique, the presented noninvasive radiographic technique does not require exposure of anatomical axis landmarks or insertion of an axis pin. This prevents additional soft-tissue trauma and potentially decreases surgical procedure time.

The findings of our study indicate that the elbow axis can be located from the lateral projection with use of fluoroscopy. This novel method of determining the elbow axis has significant clinical applications including the use of articulated external fixators, particularly hinged monolateral fixators that use a radiographic target on the fixator to align the hinge with the elbow axis. Use of such a device may increase the accuracy of alignment and decrease the technical complexity of hinge placement, as well as decrease the complication rate associated with hinged fixator placement at the elbow.

**Acknowledgment:** Financial assistance was provided by a grant from EBI Medical Systems, Parsippany, New Jersey, U.S.A.

## REFERENCES

1. Beggs JS: *Kinematics*, pp 33-49. Berlin, Springer-Verlag, 1983
2. Bottlang M, Marsh JL, Brown TD: Accuracy of screw displacement axis detection by D.C. electromagnetic motion tracking. *Trans Orthop Res Soc* 22:894, 1997
3. Bottlang M, Madey SM, Marsh JL, Brown TD: Pathway and location of instant axis of elbow rotation. *Trans Orthop Res Soc* 23:1142, 1998
4. Bottlang M, Madey SM, Steyers CM, Marsh JL, Brown TD: Hinged external elbow fixation: optimal axis alignment to minimize motion resistance. *Trans Orthop Res Soc* 24:494, 1999
5. Bottlang M, Madey SM, Steyers CM, Marsh JL, Brown TD: Assessment of elbow joint kinematics in passive motion by electromagnetic motion tracking. *J Orthop Res* 18:195-202, 2000
6. Deland JT, Garg A, Walker PS: Biomechanical basis for elbow hinge-distractor design. *Clin Orthop* 215:303-312, 1987
7. Fischer O: *Kinematik Organischer Gelenke*, pp 283-302. Braunschweig, F. Vieweg und Sohn, 1907
8. Frankle MA, Koval KJ, Sanders RW, Zuckerman JD: Radial head fractures associated with elbow dislocations treated by immediate stabilization and early motion. *J Shoulder Elbow Surg* 8:355-360, 1999
9. Hildebrand KA, Patterson SD, King GJ: Acute elbow dislocations: simple and complex. *Orthop Clin North Am* 30:63-79, 1999
10. Hotchkiss RN: *Compass Elbow Hinge, Surgical Technique*. Smith and Nephew Richards (unpublished instructional manual)
11. Kasparyan NG, Hotchkiss RN: Dynamic skeletal fixation in the upper extremity. *Hand Clinic* 13:643-663, 1997
12. London JT: Kinematics of the elbow. *J Bone Joint Surg [Am]* 63:529-535, 1981
13. McKee MD, Richards RR, Patterson SB, King GJW, Jupiter JB: The use of a dynamic, hinged, external fixator for complex, acute elbow instability. *Trans Orthop Trauma Assoc* 274-275, 1996
14. Morrey BF, Chao EYS: Passive motion of the elbow joint: a biomechanical study. *J Bone Joint Surg [Am]* 58:501-508, 1976
15. Morrey BF, Askew LJ, An KN, Chao EYS: A biomechanical study of normal functional elbow motion. *J Bone Joint Surg [Am]* 63:872-877, 1981
16. Morrey BF: Post-traumatic contracture of the elbow: operative treatment, including distraction arthroplasty. *J Bone Joint Surg [Am]* 72:601-618, 1990
17. Morrey BF: Distraction arthroplasty: clinical applications. *Clin Orthop* 293:46-54, 1993
18. Morrey BF: Current concepts in the treatment of fractures of the radial head, the olecranon, and the coronoid. Instructional Course Lecture. *J Bone Joint Surg [Am]* 44:175-185, 1995
19. Regan WD, Reilly CD: Distraction arthroplasty of the elbow. *Hand Clinic* 9:719-728, 1993
20. Shiba R, Sorbie C, Siu DW, Bryant JT, Cook TD, Wevers HW: Geometry of the humeroulnar joint. *J Orthop Res* 6:897-906, 1988
21. Tanaka S, An KN, Morrey BF: Kinematics and laxity of ulno-humeral joint under varus-valgus stress. *J Musculoskel Res* 2:45-54, 1998
22. Volkov MV, Oganesian OV: Restoration of function in the knee and elbow with a hinge-distractor apparatus. *J Bone Joint Surg [Am]* 57:591-600, 1975
23. Von Meyer H: The mechanics of the elbow joint. In: *Kinesiology of the Human Body under Normal and Pathologic Conditions*, pp 490-507. By A Steindler. Springfield, Illinois, Charles C. Thomas, 1955
24. Wyrsh RB, Seiler JG, Weikert DR, Murray D, Wyrick J, Stern PJ: Early experience with the compass elbow hinge: a retrospective review. *Orthop Trans* 21:442, 1997